DOI: 10.5604/01.3001.0015.0517
Volume 105 • Issue 2 • April 2021
Journal of Achievements in Materials and Manufacturing Engineering
International Scientific Journal published monthly by the World Academy of Materials and Manufacturing Engineering

# Bearing capacity of E-shaped footing on layered sand

**S. Nazeer [a], R.K. Dutta [b,*]**
[a] PG Student, Department of Civil Engineering, National Institute of Technology, Hamirpur, India
[b] Professor, Department of Civil Engineering, National Institute of Technology, Hamirpur, India
* Corresponding e-mail address: rkd@nith.ac.in
ORCID identifier: https://orcid.org/0000-0002-4611-9950 (R.K.D.)

## ABSTRACT

**Purpose:** The purpose of this study is to estimate the ultimate bearing capacity of the E-shaped footing resting on two layered sand using finite element method. The solution was implemented using ABACUS software.

**Design/methodology/approach:** The numerical study of the ultimate bearing capacity of the E-shaped footing resting on layered sand and subjected to vertical load was carried out using finite element analysis. The layered sand was having an upper layer of loose sand of thickness *H* and lower layer was considered as dense sand of infinite depth. The various parameters varied were the friction angle of the upper (30° to 34°) and lower (42° to 46°) layer of sand as well as the thickness (0.5*B*, 2*B* and 4*B*) of the upper sand layer.

**Findings:** The results reveal that the dimensionless ultimate bearing capacity was found to decrease with the increased in the *H/B* ratio for all combinations of parameters. The dimensionless ultimate bearing capacity was maximum for the upper loose sand friction angle of 34° and lower dense sand friction angle of 46°. The results further reveal that the dimensionless bearing capacity of the E-shaped footing was higher in comparison to the dimensionless bearing capacity of the square footing on layered sand (loose over dense). The improvement in the ultimate bearing capacity for the E-shaped footing was observed in the range of 109.35% to 152.24%, 0.44% to 7.63% and 0.63% to 18.97% corresponding to *H/B* ratio of 0.5, 2 and 4 respectively. The lowest percentage improvement in the dimensionless bearing capacity for the E-shaped footing on layered sand was 0.44 % at a *H/B* = 2 whereas the highest improvement was 152.24 % at a *H/B* = 0.5. Change of footing shape from square to E-shaped, the failure mechanism changes from general shear to local shear failure.

**Research limitations/implications:** The results presented in this paper were based on the numerical study conducted on E-shaped footing made out of a square footing of size 1.5 m x 1.5 m. However, further validation of the results presented in this paper, is recommended using experimental study conducted on similar size E-shaped footing.

**Practical implications:** The proposed numerical study can be useful for the architects designing similar types of super structures requiring similar shaped footings.

**Originality/value:** No numerical study on E-shaped footing resting on layered sand (loose over dense) were conducted so far. Hence, an attempt was made in this article to estimate the bearing capacity of these footings.

**Keywords:** Square footing, E-Shaped footing, Finite-element analysis, Bearing capacity, Layered sand, Thickness of upper layer, Friction angle

**Reference to this paper should be given in the following way:**
S. Nazeer, R.K. Dutta, Bearing capacity of E-shaped footing on layered sand, Journal of Achievements in Materials and Manufacturing Engineering 105/2 (2021) 49-60.
DOI: https://doi.org/10.5604/01.3001.0015.0517

ANALYSIS AND MODELLING

## 1. Introduction

In the foundation design, conventional shapes of the footings such as square, rectangular, strip, circular or ring were used since long. Due to architectural requirements, asymmetric plan shaped multi-story buildings are becoming increasingly popular. For these types of footings, there are no bearing capacity calculation methods in the codes of practice are available. As a result, in order to predict the bearing capacity of these types of footings, researchers must use either experimental or numerical methods. These footings are known as multi-edge footings as they have more than four edges and are built to safely and economically transfer the load from an asymmetric shaped structure to the underlying soils. In addition, it is well established that shear failure followed by a large settlement occurs for the footing resting on loose sand. In this situation, the densification of the sand to a certain depth is carried out in order to increase the bearing capacity. Contrary to this, due to the incorrect investigation of the subsurface, the presence of loose sand over the dense sand layer can sometimes be ignored. In each of the above cases, it is important to take into account the effect of the loose sand overlying the dense sand layer on the bearing capacity of the footing. Appreciable work for the conventional shaped footings resting on single or two layered soils [1-23] was available in literature. Studies were also reported in literature [1, 19-21, 24-28] for the multi-edge footings resting on single layer of soil. Laboratory tests reported by [19] on a square and H-shaped footing reveals that the development of shear zones in between the multi-edges, led to passive force generation in the other parts and thus require more load to extend the shear zone in larger areas and thus, to cause failure in the soil. Study reported by [25] on Plus, H, T and square shaped footings concluded that the load increases with an increase in the footing size for loose as well as dense sand. The authors further concluded that the failure load and settlement for these footings remain almost constant when resting on loose sands whereas failure load and settlement started decreasing and increasing for the dense sand respectively. 3D numerical study reported by [26] concluded that the bearing capacity ratio were greater for the multi-edge footings in comparison to the square footing of the same width. Further, the experimental and numerical studies on conventional and multi-edge shaped footings resting on single layer of soil were reported in literature [1, 19-21, 24-28]. These studies have used steel as a footing material. But practically, concrete was always user's choice as a construction material. Hence, there is scarcity of the data about multi-edge footings resting on layered soils. Therefore, this research work regarding E-shaped footing resting on layered soil was taken up to fill this gap. The paper presents the numerical study on the ultimate bearing capacity of the E-shaped footing resting on loose sand overlying dense sand deposit.

## 2. Problem definition and model parameters

An E-shaped footing subjected to a vertical concentric load resting on loose sand overlying dense sand was used for modelling as shown in Figure 1. The thickness (H) of the upper loose sand layer was varied from 0.5B to 4B and that of the lower dense sand was considered of infinite depth. The parameters varied were unit weight of upper loose sand layer ($\gamma 1$) and lower dense sand layer ($\gamma 2$), friction angle of upper ($\phi 1$) and lower ($\phi 2$) layer of sand. The modulus of elasticity, Poisson ratio and dilation angle of the upper layer of loose sand ($E_1$, $\mu_1$, $\psi_1$) and lower dense sand ($E_2$, $\mu_2$, $\psi_2$) layer were considered in the study. The unit weight of the upper loose ($\gamma_1$) and lower dense sand layer ($\gamma_2$) were varied as 13.5 kN/m$^3$ to 15.0 kN/m$^3$ and 18 kN/m$^3$ to 20 kN/m$^3$ respectively. The friction angle of the upper loose sand ($\phi_1$) and lower dense sand ($\phi_2$) layer were varied from 30°to 34° and 42° to 46° respectively. These friction angles were taken corresponding to the unit weight of the sand as per [29]. The modulus of elasticity and the Poisson ratio for the upper loose sand layer ($E_1$, $\mu_1$) and the lower dense sand layer ($E_2$, $\mu_2$) were taken as 18000 kN/m$^3$ , 0.3 and 65000 kN/m$^3$ , 0.34 respectively as per [30] for modelling for all the combinations studied. The dilation angle ($\psi$) for both the layers of sand was calculated using $\varphi$-30° as per [23] for modelling and their values are tabulated in Table 1. For modelling, the vertical load was applied at the centre of the square as well as E-shaped footing as shown in Figure 2. The density ($\gamma$), modulus of elasticity (E) and the Poisson ratio ($\upsilon$) of the concrete was taken as 24 kN/m$^3$, 30 GPa and 0.25 respectively for the footing material as per [31-32].

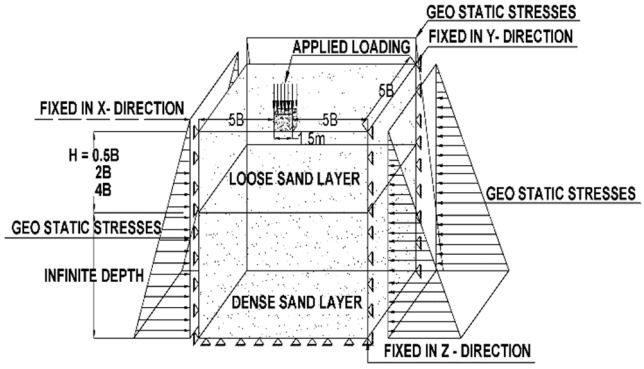


Fig. 1. Problem domain and boundary conditions

Table 1.
Dilation angles used for modelling

| Friction angle, Deg. | Dilation angle, Deg. |
|---|---|
| 30 | 0 |
| 32 | 2 |
| 34 | 4 |
| 42 | 12 |
| 44 | 14 |
| 46 | 16 |

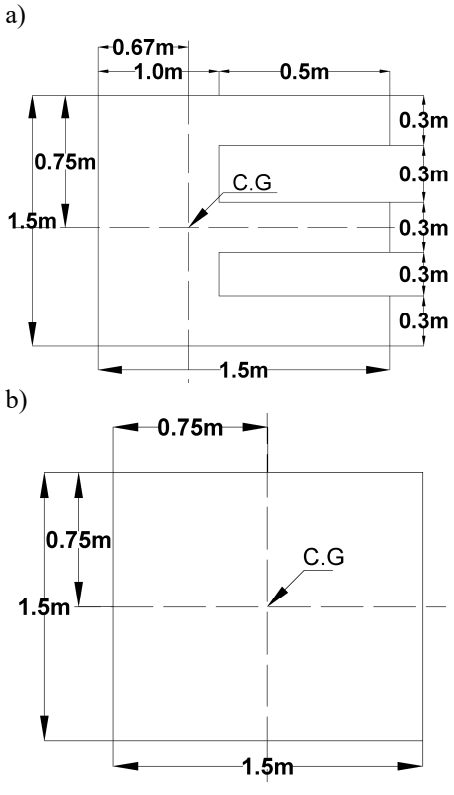


Fig. 2. Location of centre of gravity for (a) E-shaped footing (b) square footing

## 3. Finite element meshing and boundary conditions

Commercially available ABACUS software was used for the study of the pressure settlement behaviour of the square as well as E-shaped footing. The dimension of the square footing considered for modelling was 1.5 m x 1.5 m x1.0 m as per [9-10]. The E-shaped footing was made out of the square footing of size 1.5 m x 1.5 m as shown in Figure 2.

The Mohr-Coulomb model was used for the analysis. This model represents the 'first order' approximation of the sand behaviour by estimating a constant average stiffness that led to faster computations to obtain first estimate of the deformations whereas the other soil hardening models take more computational time [1]. The nature of the soil-elements was assumed to be elasto-plastic. The element used for modelling was C3D8R. Vertical loading was applied to the footing which transfers the load to the underlying two layered strata. The two layered soil model having dimensions of 5B from footing edge in the x, y and z direction was created. This was done to avoid the boundary effects and to stimulate the actual ground conditions. Near the vertical axis of the footing, the meshing was finer which changed to coarser as the distance from the footing edge increased as shown in the Figure 3. Geostatic stress was also applied before the application of the vertical loading as shown in Figure 1. It was observed that the greater number of elements in the mesh leads to the improvement in ultimate bearing capacity by 2-7% but the time required for simulating the same becomes two folds. The convergence study reveals that the optimal number of elements obtained in the present study was 31520. Beyond this range, there was not an appreciable change in the ultimate bearing capacity of model footings. Figure 3 represents the basic meshing for a square shaped and E-shaped footing used in the analysis.

## 4. Software validation

In order to validate the software, it was thought to perform an additional analysis using the experimental data for the square footing resting on single layer of sand and reported by [27]. The parameters considered for the validation were the relative density of sand (30%, 50%, 70% and 87%), unit weight of sand (13.87 kN/m$^3$, 14.44 kN/m$^3$, 15.04 kN/m$^3$ and 15.54 kN/m$^3$) and friction angle (36.5°, 40.1°, 42.05° and 44.6°). It is pertinent to mention here that [19] reported a friction angle obtained through triaxial testing corresponding to a relative density of 30%, 40%, 50%, and 60% as 36.06°, 38.64°, 39.86°, and 41.72° respectively, hence the friction angle of the sand chosen for modelling are justifiable.

a)

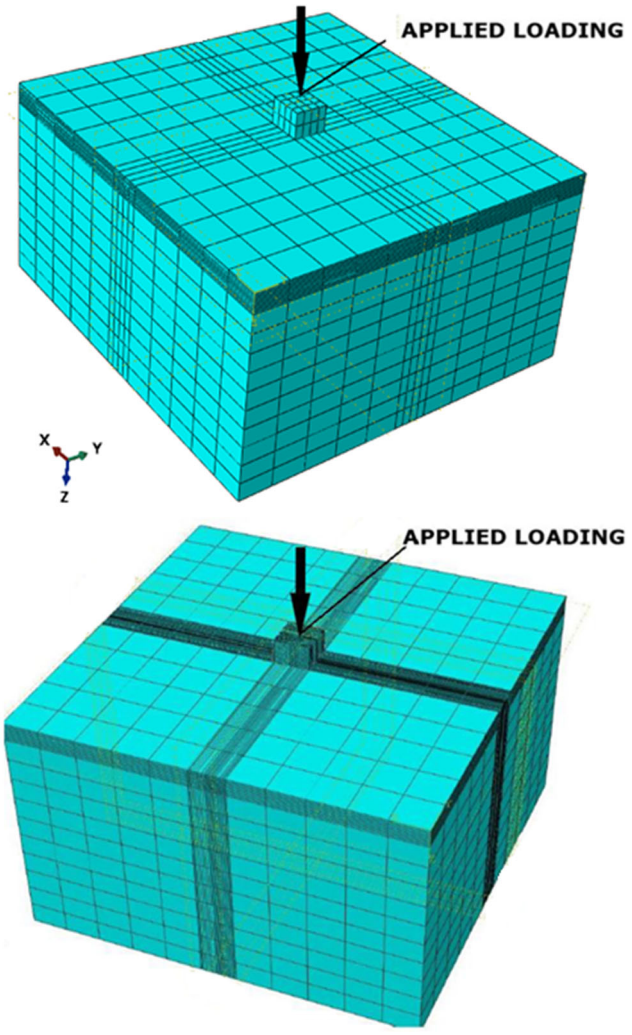


Fig. 3. Meshing of (a) square footing and (b) E-shaped footing resting on layered sand

The internal friction angle between the steel and soil was taken as 22°, 24.2°, 25.5° and 26.9° respectively corresponding to a relative density of 30%, 50%, 70% and 87% for modelling. The dimensions of the model considered were 700 mm x 450 mm x 600 mm. Footing of size 50 mm x 50 mm x 10 mm was used for the validation. The data for the modulus of elasticity and Poisson ratio of the sand was not reported in [28]. The same were taken as 18 MPa and 0.3 respectively as reported by [30] for the sand for modelling. The density of steel, modulus of elasticity and Poisson ratio of the footing material were taken as 78.50 kN/m$^3$, 210 GPa and 0.303 as per [33]. The comparison of the results is shown in Table 2. Study of Table 2 reveals that the average deviation in the bearing capacity was 10.2 % corresponding to the different relative densities. This deviation is attributed to the use of empirical correlations in deriving the principal parameters of the sand considered for modelling.

Table 2.
Comparison of the results for the software validation

| Bearing capacity (qu) at s/B ratio of 10% | | |
|---|---|---|
| R.D, % | Khatri et al [28] | Present work |
| 30 | 34.80 | 23.94 |
| 50 | 52.00 | 44.50 |
| 70 | 70.20 | 61.34 |
| 87 | 88.20 | 101.83 |

## 5. Codification

For easy reference and apprehensibility, specific codification was used in graphs. The codification S-XX-YY-ZZ was used for representing square/E-shape footing (S or E) followed by the friction angle of upper loose sand layer (XX represents 30°, 32°, 34°),friction angle of lower dense sand layer (YY represents 42°, 44°, 46°) and H/B ratio (ZZ represents 0.5, 2,4) respectively.

## 6. Results and discussions

Figure 4 presents the typical pressure-settlement ratio plots obtained from the numerical study. The ultimate bearing capacity was obtained by taking the minimum of peak pressure or pressure corresponding to the s/B ratio of 10%, whichever occur earlier as per [34]. If the peak is not clearly observed, then double tangent method was used to calculate the same. After the validation of software, the numerical study was carried out by varying the thickness of the upper layer from 0.5B to 4B, friction angle of the upper layer from 30° to 34° and the friction angle for the lower dense sand from 42° to 46°. The results thus obtained from the study are presented in the following sections.

### 6.1. Effect of H/B on dimensionless ultimate bearing capacity

In order to study the effect of thickness of the upper loose sand layer on the dimensionless bearing capacity ($q_u/\gamma B$), the results are presented in Figure 5 and Table 3. Study of this figure reveals that for the E-shaped footing, the dimensionless bearing capacity decreased with the increase in the H/B ratio. This is attributed to the fact that the effect of vertical load diminishes or becomes negligible beyond a depth of 2B for different shapes of footing as per [6].

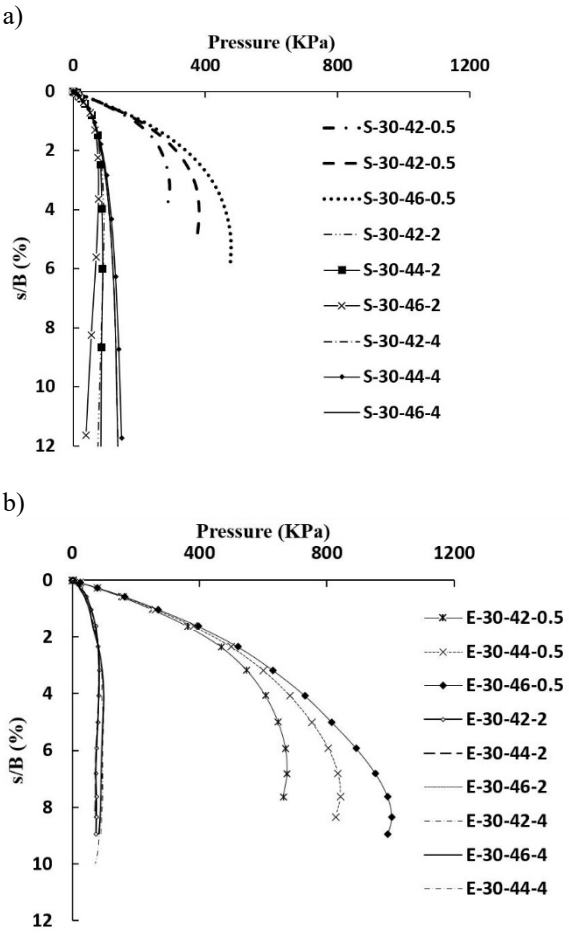


Fig. 4. Pressure settlement ratio plot for the footing (a) Square (b) E-shaped on layered sand at $\varphi_1 = 30°$ and $\varphi_2 = 42°, 44°, 46°$ corresponding to different H/B ratio

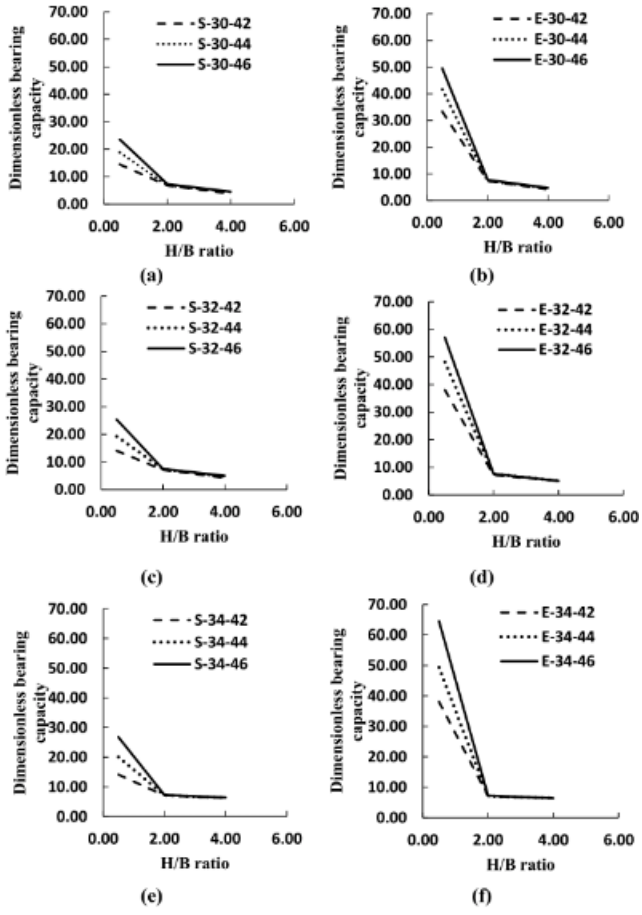


Fig. 5. Dimensional ultimate bearing capacity versus H/B curves for loose sand layer friction angle of $\varphi_1 = 30°, 32°, 34°$ (a),(c),(e) for square footing (b), (d), (f) for E-shaped footing on layered sand

Table 3.
Dimensionless bearing capacity obtained from the present study

| ϕ1 | ϕ2 | Dimensionless bearing capacity ($q_u/\gamma_1 B$) | | | | | |
|---|---|---|---|---|---|---|---|
| | | Square footing | | | E-shaped footing | | |
| | | H=0.5B | H=2B | H=4B | H=0.5B | H=2B | H=4B |
| 30 | 42 | 14.46 | 6.78 | 3.79 | 33.33 | 7.29 | 4.20 |
| 30 | 44 | 18.82 | 6.79 | 4.44 | 41.57 | 7.28 | 4.70 |
| 30 | 46 | 23.54 | 7.26 | 4.58 | 49.55 | 7.74 | 4.72 |
| 32 | 42 | 14.06 | 7.13 | 4.27 | 38.09 | 7.20 | 5.08 |
| 32 | 44 | 19.31 | 7.49 | 4.71 | 48.18 | 7.64 | 5.08 |
| 32 | 46 | 25.39 | 7.49 | 5.05 | 57.08 | 7.65 | 5.09 |
| 34 | 42 | 14.14 | 7.13 | 6.28 | 38.09 | 7.17 | 6.39 |
| 34 | 44 | 20.07 | 7.15 | 6.33 | 49.37 | 7.18 | 6.40 |
| 34 | 46 | 26.76 | 7.25 | 6.38 | 64.56 | 7.29 | 6.42 |

Further study of this figure reveals that the decrease in the dimensionless bearing capacity was appreciable up to a H/B ratio of 2. Beyond this, the change in the dimensionless bearing capacity was marginal indicating almost negligible contribution of the lower dense sand layer. The above mentioned trend was similar for all combinations of friction angle of lower and upper sand layers with the increase in the H/B ratio.

Comparison

The comparison of the results obtained from the numerical study presented in Figure 5 and Table 3 reveals that corresponding to the same H/B ratio as well as friction angle, the dimensionless bearing capacity in case of E-shaped footing was higher in comparison to the square footing. The highest (152.24%) and the lowest (0.44%) increase in the dimensionless bearing capacity were observed in case of H/B ratio of 0.5 and 4 respectively. The higher improvement in the dimensionless bearing capacity in case of E-shaped footing in comparison to the square footing is in agreement with the literature [24,26].

Vectorial displacement

Typical vectorial displacement for the E-shaped and square footing resting on upper loose sand ($\phi_1$=30°) overlying lower dense sand layer ($\phi_2$=42°, 44°, 46°) corresponding to different H/B ratios were shown in Figure 6.

Study of Figure 6 reveals that the vectorial displacement vector enters the lower dense sand layer for H/B ratio of 0.5 and 2. The trend was similar for the square and E-shaped footing for all combinations of friction angles. Further study of Figure 6 reveals that for the E-shaped footing, loose sand participates up to a larger depth in comparison to the square footing. This concludes that the ultimate bearing capacity depends up on the properties of both the upper loose and lower dense layers up to H/B equal to 2. It can be further observed that there is a punching shear failure in both the footings with considerable settlement for all the cases.

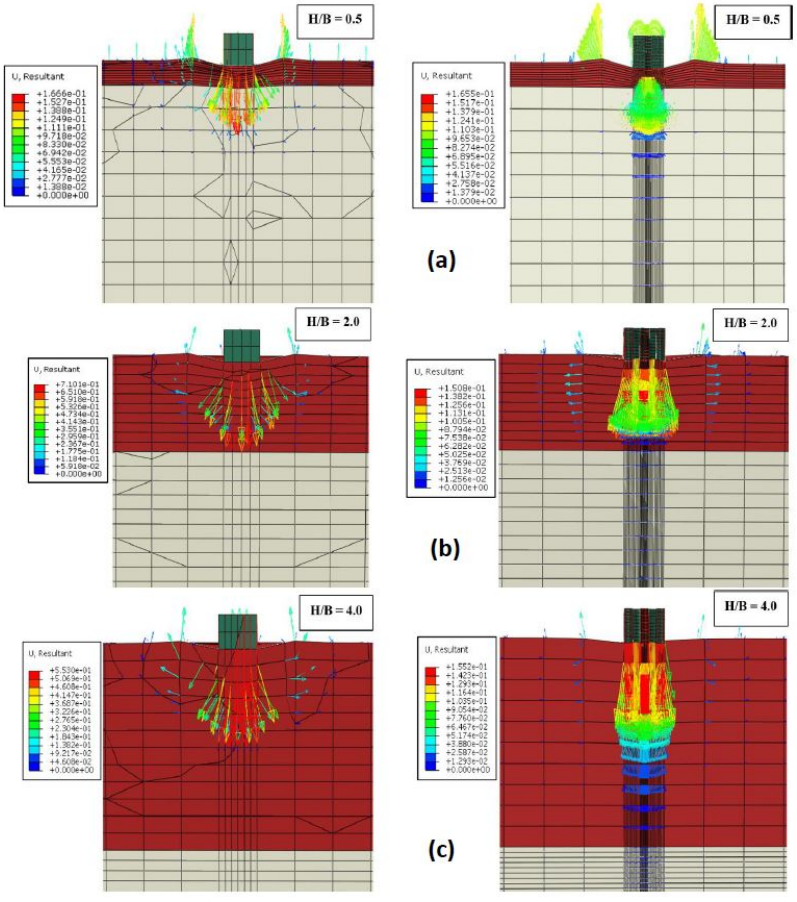


Fig. 6. Vectorial displacement of layered sand at different H/B ratio for regular square footing (left) and E-shaped footing (right) friction angle of $\varphi_1$ = 30° and $\varphi_2$ = 46° respectively

### 6.2. Effect of friction angle of upper loose (ϕ1) and lower dense (ϕ2) sand layer on the ultimate bearing capacity

The results of the effect of the friction angle of the upper loose and lower dense sand layer which was varied from 30° to 34° and 42° to 46° respectively were presented in Figures 7 to 9.

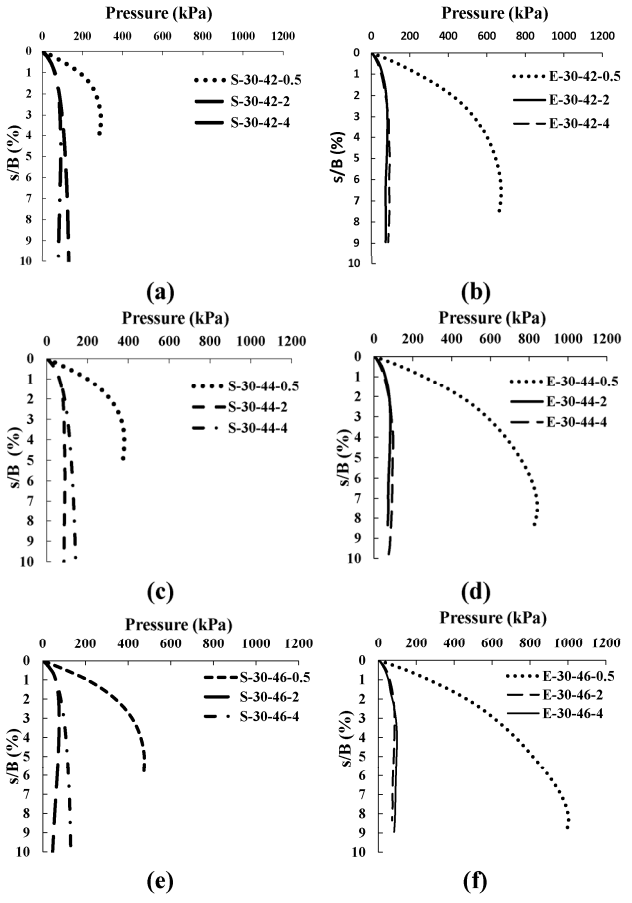


Fig. 7. Pressure-settlement ratio plot for regular square shaped footing (left) and E-shaped footing (right) at $\varphi_1 = 30°$ and $\varphi_2 = 42°,44°,46°$respectively

From these Figures, it was observed that with the increase in the friction angle of the lower dense sand layer, the ultimate bearing capacity increased at a constant friction angle of the upper loose sand layer. Likewise, with the increase in friction angle of upper loose sand layer, the ultimate bearing capacity increased at a constant friction angle of the lower dense sand layer. This is attributed to the fact that increases in the friction angle of lower loose or

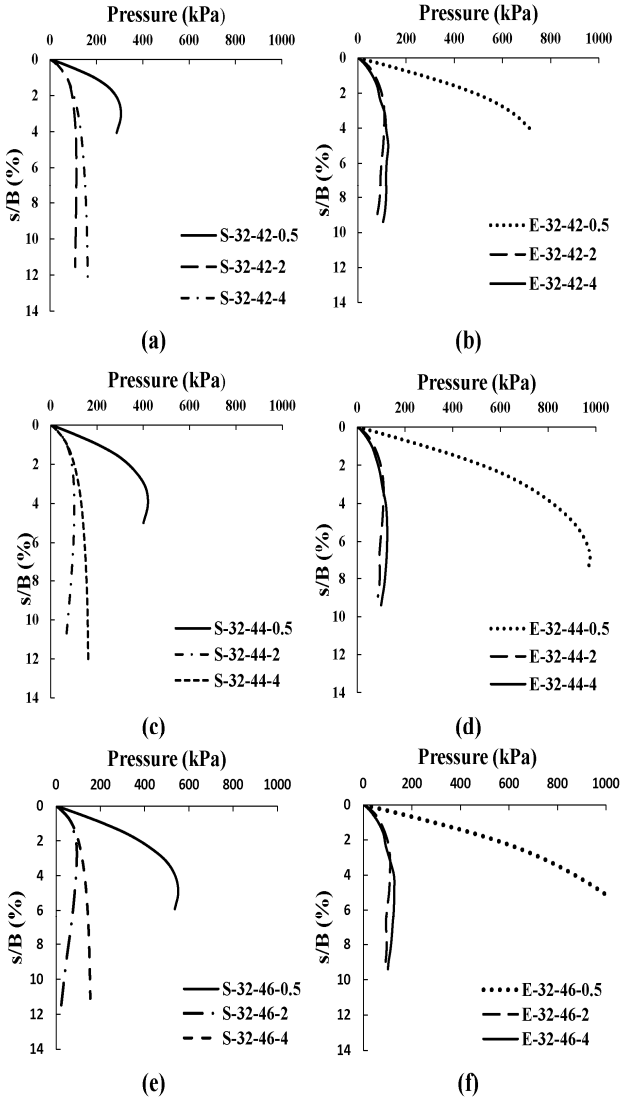


Fig. 8. Pressure-settlement ratio plot for regular square shaped footing (left) and E-shaped footing (right) at $\varphi_1 = 32°$ and $\varphi_2 = 42°$, 44°, 46°respectively

upper dense sand layer results in increase in the ultimate bearing capacity. Further study of Figures 7 to 9 reveals that the ultimate bearing capacity for the E-shaped footing was higher in comparison to the square footing. The percentage improvement in the numerically obtained dimensionless bearing capacity for the E-shaped footing is tabulated in Table 4. A close examination of this table reveals that the improvement in the dimensionless bearing capacity was of the order of 109.35% to 152.24%, 0.44% to 7.63% and 0.63% to 18.97% corresponding to a *H/B* ratio of 0.5, 2.0 and 4.0 respectively. Further, study of Table 4 reveals that

the lowest percentage improvement in the dimensionless bearing capacity for the E-shaped footing on layered sand was 0.44 % at a $H/B$ = 2 whereas the highest improvement was 152.24 % at a $H/B$ = 0.5.

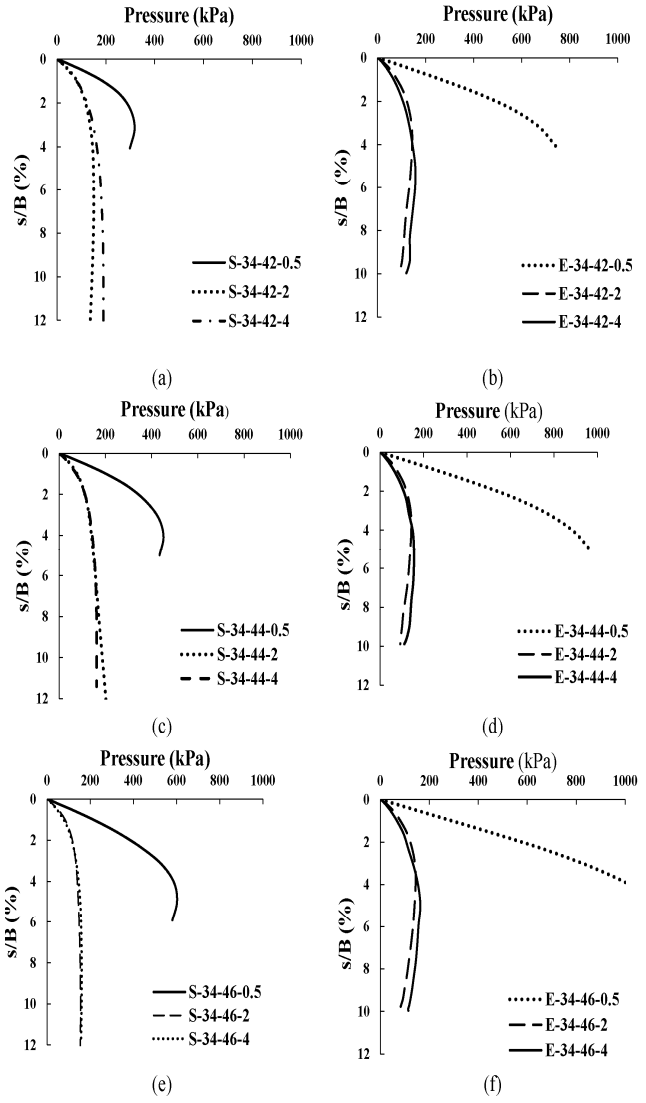


Fig. 9 Pressure-settlement ratio plot for regular square shaped footing (left) and E-shaped footing (right) at $\varphi_1$ = 34° and $\varphi_2$ = 42°, 44°, 46°respectively

This improvement in the dimensionless bearing capacity is attributed to the change in the geometry of the footing resulting higher ultimate bearing capacity for the E-shaped footing resting on layered sand.

Table 4.
Percentage improvement in the dimensionless bearing capacity

| Percentage improvement in the dimensionless bearing capacity | | | |
|---|---|---|---|
| $\phi_1$, $\phi_2$ | H=0.5B | H=2B | H=4B |
| 30, 42 | 130.58 | 7.63 | 11.00 |
| 30, 44 | 120.91 | 7.22 | 5.92 |
| 30, 46 | 110.52 | 6.59 | 3.22 |
| 32, 42 | 152.24 | 1.06 | 18.97 |
| 32, 44 | 132.23 | 2.09 | 7.89 |
| 32, 46 | 109.35 | 2.19 | 0.81 |
| 34, 42 | 142.46 | 0.61 | 1.88 |
| 34, 44 | 121.42 | 0.44 | 1.05 |
| 34, 46 | 117.15 | 0.60 | 0.63 |

### 6.3. Failure patterns

Figure 10 presents the failure patterns below the E-shaped and square shaped footing at $\phi_1$ = 30° and $\phi_2$ = 42° corresponding to H/B ratio of 4.0. The failure patterns shown in this figure corresponds to the various sections (as shown in Fig. 10a) of the E-shaped footing are depicted in Figure 10b to Figure 10g. Figure 10h presents the failure pattern for the square shaped footing at its mid-section. Study of Figure 10b to Figure 10h reveals that the plastic strain is greater than zero which signifies that the soil material has yielded below the base of the footing in all the sections. However, the lowest plastic strain was observed below the base of the square shaped footing (Fig. 10h) while the highest plastic strain was observed below the base of the E-shaped footing corresponding to sections $X_3$-$X_4$ and $Y_5$-$Y_6$ as evident in, Figure 10d and Figure 10g respectively. The failure patterns observed in Figure 10b, Figure 10c, and Figure 10d were similar with no occurrence of heaving at the ground surface indicating a local shear failure. The failure surfaces extend to the ground surface in Figure 10e and Figure 10f, but no heave was detected, indicating local shear failure in this case, but the failure pattern was different from the previous case. In contrast to the rest of the sections provided for E-shaped footing, there were stress concentrations at the edges of the E-shape in Figure 10g.

Heaving, on the other hand, was not noticed in this section. The soil beneath the footing was more stressed than the soil around it. As a result, the local shear failure pattern governed the E-shaped footing's ultimate bearing capacity, and the slip surface was well defined. Furthermore, Figure 10h shows a well-defined failure surface extending up to ground level, as well as bulging of the ground surface adjacent to the footing prior to failure, resulting in a general shear failure.

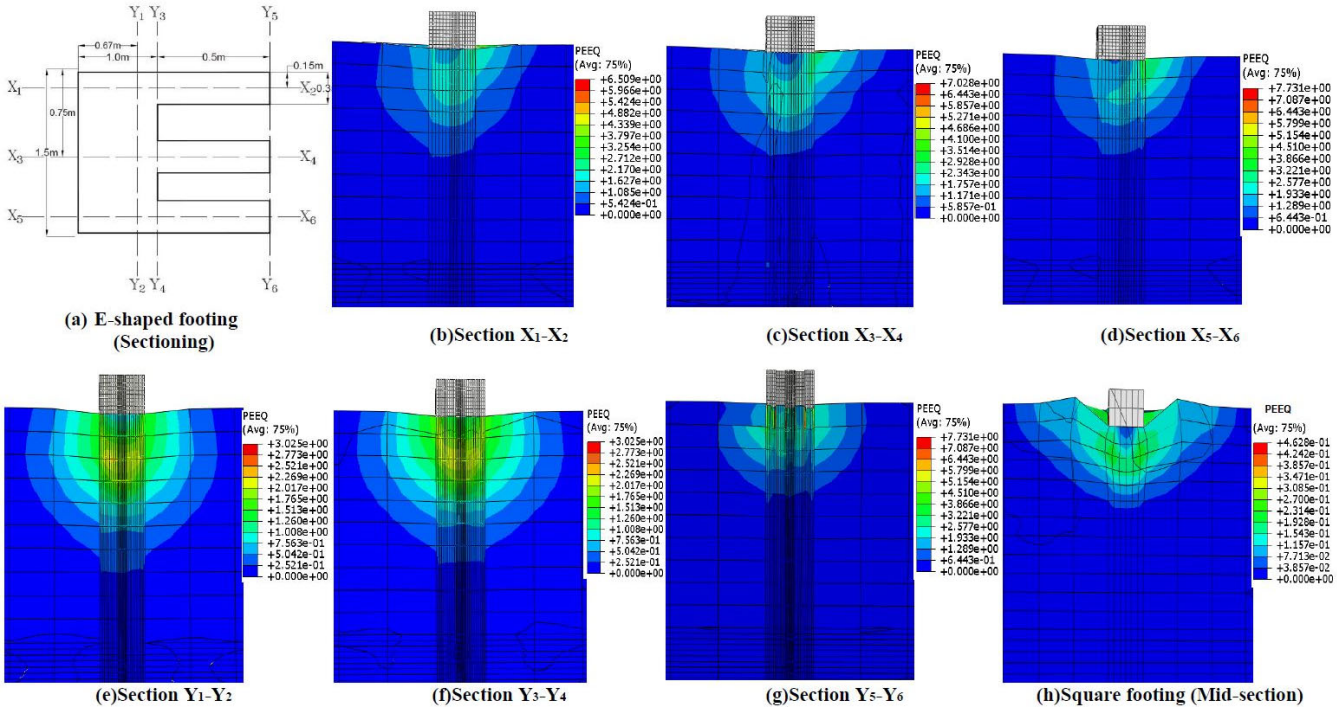


Fig. 10. Failure pattern below the E-shaped footing and Square shaped footing at $\varphi_1 = 30°$ and $\varphi_2 = 42°$ corresponding to H/B ratio of 4.0

As a result of the foregoing observations, it can be concluded that when the footing shape changes from square to E-shaped, the failure mechanism switches from general shear failure to local shear failure. The failure patterns discovered in the above study will be useful in designing analytical solutions.

### 6.4. Displacement contours

Typical displacement contours for selected values of H/B ratio of 0.5, 2 and 4 and varying the friction angle of lower dense sand from 42° to 46° and keeping constant friction angle of upper loose sand layer are presented in Figure 11. This Figure show the total contour of the displacement and their importance is to assess the actual displacement under the load. This type of information is required in order to verify the vertical settlement in the footing design within the acceptable limits or not under the load. Analysis of this figure reveals that the isobar distance for the E-shaped footing is greater than for the square footing at a H/B ratio of 0.5, 2 and 4, indicating a higher ultimate bearing capacity for the former. In addition, the analysis of this figure indicates that the displacement contours remained well established within the selected lateral and vertical distance for the E-shaped and the square footings corresponding to a H/B ratio of 0.5, 2 and 4. This means it was enough for the chosen problem domain. The insights gained from the above study on the displacement contours will be useful for developing analytical solutions.

## 7. Conclusions

The numerical study on the E-shaped and square footing resting on upper loose sand overlying lower dense sand layer and subjected to vertical concentric load is investigated. A series of numerical analysis was performed to assess the E-shaped and square footings resting on loose sand layer overlying dense sand layer. From the results and discussion presented above, the following conclusions are drawn:

1. The ultimate bearing capacity was higher for the E-shaped footing in comparison to the square footing for all combinations of parameters studied.
2. The improvement in the ultimate bearing capacity for the E-shaped footing was observed in the range of 109.35 % to 152.24 %, 0.44 % to 7.63 % and 0.63 % to 18.97% corresponding to H/B ratio of 0.5, 2 and 4 respectively.
3. The lowest percentage improvement in the dimensionless bearing capacity for the E-shaped footing

on layered sand was 0.44 % at a H/B = 2 whereas the highest improvement was 152.24 % at a H/B = 0.5.

4. The dimensionless ultimate bearing capacity was the maximum for the upper loose and lower dense sand friction angles of 34° and 46° respectively while it was the lowest for the upper loose and lower dense sand corresponding to the friction angle of 30° and 42°.
5. Change of footing shape from square to E-shaped, the failure mechanism changes from general shear to local shear failure.
6. The displacement contours generated supports the observations of the E-shaped and square footings with regard to the ultimate bearing capacity on layered sands.
7. The results presented in this paper were based on numerical analysis. However, for the actual footings the soil placement, compaction and details of the stress level will be different from the numerical analysis. Further investigations using full-scale experimental field size footings were recommended to generalize the results.

## Notations

| | |
|---|---|
| B | Width of footing |
| H | Thickness of the upper loose sand layer |
| s | Settlement of footing |
| s/B | Normalized settlement |
| $\gamma_1$ | Unit weight of upper loose sand layer |
| $\gamma_2$ | Unit weight of lower dense sand layer |
| $\phi_1$ | Friction angle of upper loose sand |
| $\phi_2$ | Friction angle of lower dense sand |
| $\mu_1$ | Poisson ratio of upper loose sand layer |
| $\mu_2$ | Poisson ratio of lower dense sand layer |
| $E_1$ | Modulus of elasticity of upper loose sand layer |
| $E_2$ | Modulus of elasticity of lower dense sand layer |
| $\Psi_1$ | Dilation angle of upper loose sand layer |
| $\Psi_2$ | Dilation angle of lower dense sand layer |
| H/B | Thickness ratio |
| $q_u$ | Ultimate bearing capacity |
| $q_u/\gamma_1 B$ | Dimensionless ultimate bearing capacity |

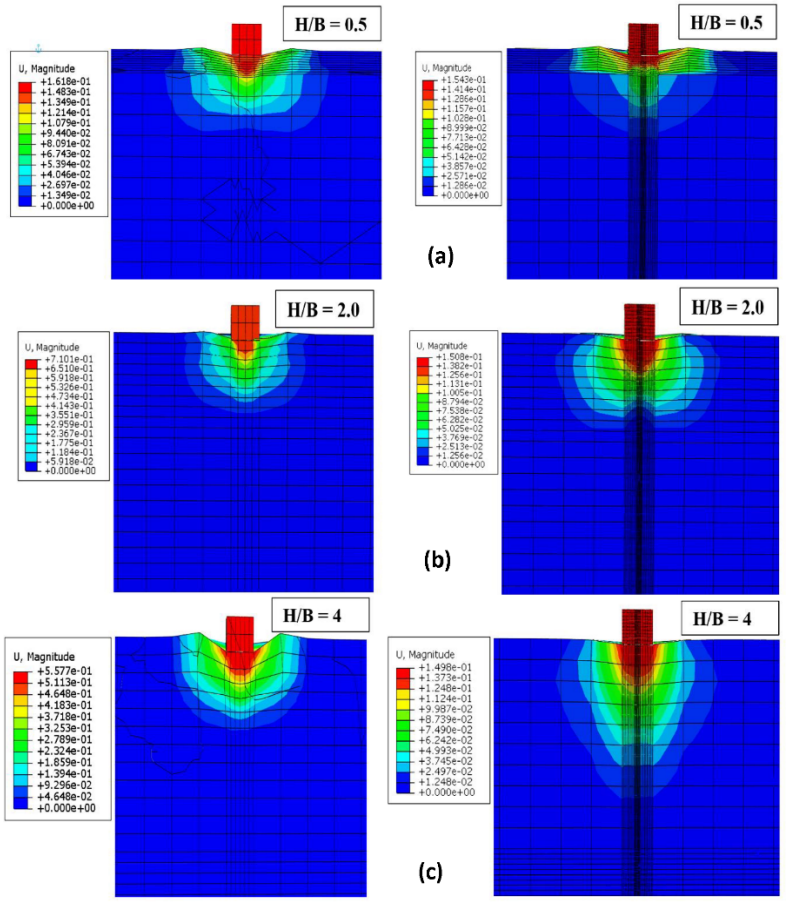


Fig. 11. Displacement contours of layered sand at different H/B ratio for regular square footing (left) and E-shaped footing (right) friction angle of φ1 = 30° and φ2 = 46° respectively

## Acknowledgements

I would like to express my special thanks of gratitude to Central Building Research Institute (CSIR-CBRI) Roorkee for providing me the opportunity to utilize the ABACUS software.

## References

[1] A. Thakur, R.K. Dutta, Experimental and numerical studies of skirted hexagonal footings on three sands, SN Applied Sciences 2/3 (2020) 487. DOI: https://doi.org/10.1007/s42452-020-2239-9

[2] A. Thakur, R.K. Dutta, A study on bearing capacity of skirted square footings on different sands, Indian Geotechnical Journal 50/6 (2020) 1057-1073. DOI: https://doi.org/10.1007/s40098-020-00440-4

[3] A.K. Nazir, W.R. Azzam, Improving the bearing capacity of footing on soft clay with sand pile with/without skirts, Alexandria Engineering Journal 49/4 (2010) 371-377. DOI: https://doi.org/10.1016/j.aej.2010.06.002

[4] A.Z. El Wakil, Horizontal capacity of skirted circular shallow footings on sand, Alexandria Engineering Journal 49/4 (2010) 379-385. DOI: https://doi.org/10.1016/j.aej.2010.07.003

[5] A.Z. EL Wakil, Bearing capacity of skirt circular footing on sand, Alexandria Engineering Journal 52/3 (2013) 359-364. DOI: https://doi.org/10.1016/j.aej.2013.01.007

[6] A.M. Hanna, Finite element analysis of footings on layered soils, Mathematical Modelling 9/11 (1987) 813-819. DOI: https://doi.org/10.1016/0270-0255(87)90501-X

[7] A.M. Hanna, Bearing capacity of foundations on a weak sand layer overlying a strong deposit, Canadian Geotechnical Journal 19/3 (1982) 392-396. DOI: https://doi.org/10.1139/t82-043

[8] A. Mosadegh, H. Nikraz, Bearing capacity evaluation of footing on a layered-soil using ABAQUS, Journal of Earth Science & Climatic Change 6/3 (2015) 1000264. DOI: https://doi.org/10.4172/2157-7617.1000264

[9] A. Gupta, R.K. Dutta, R. Shrivastava, V.N. Khatri, Ultimate bearing capacity of square/rectangular footing on layered soil, Indian Geotechnical Journal, 47/3 (2017) 303-313. DOI: https://doi.org/10.1007/s40098-017-0233-y

[10] V.C. Joshi, R.K. Dutta, R. Shrivastava, Ultimate bearing capacity of circular footing on layered soil, Journal of Geoengineering 10/1 (2015) 25-34. DOI: http://dx.doi.org/10.6310%2fjog.2015.10(1).4

[11] G.G. Meyerhof, Ultimate bearing capacity of footings on sand layer overlying clay, Canadian Geotechnical Journal 11/2 (1974) 223-229. DOI: https://doi.org/10.1139/t74-018

[12] H.T. Eid, Bearing capacity and settlement of skirted shallow foundations on sand, International Journal of Geomechanics 13/5 (2013) 645-652. DOI: https://doi.org/10.1061/(ASCE)GM.1943-5622.0000237

[13] H.T. Eid, O.A. Alansari, A.M. Odeh, M.N. Nasr, H.A. Sadek, Comparative study on the behavior of square foundations resting on confined sand, Canadian Geotechnical Journal 46/4 (2009) 438-453. DOI: https://doi.org/10.1139/T08-134

[14] J.S. Shiau, A.V. Lyamin, S.W. Sloan, Bearing capacity of a sand layer on clay by finite element limit analysis, Canadian Geotechnical Journal 40/5 (2003) 900-915. DOI: https://doi.org/10.1139/t03-042

[15] K. Johnson, M. Christensen, N. Sivakugan, W. Karunasena, Simulating the response of shallow foundations using finite element modelling, Proceedings of the MODSIM 2003 International Congress on Modelling and Simulation, Townsville, QLD, Australia, 14-17 July 2003, 2060-2065.

[16] M. Georgiadis, A. Michalopoulos, Bearing capacity of gravity bases on layered soil, Journal of the Geotechnical Engineering 111/6 (1985) 712-729. DOI: https://doi.org/10.1061/(ASCE)0733-9410(1985)111:6(712)

[17] M.J. Kenny, K.Z. Andrawes, The bearing capacity of footings on a sand layer overlying soft clay, Géotechnique 47/2 (1997) 339-345. DOI: https://doi.org/10.1680/geot.1997.47.2.339

[18] M.D. Shoaei, A. Alkarni, J. Noorzaei, M.S. Jaafar, B.B.K. Huat, Review of available approaches for ultimate bearing capacity of two-layered soils, Journal of Civil Engineering and Management 18/4 (2012) 469-482. DOI: https://doi.org/10.3846/13923730.2012.699930

[19] T. Gnananandarao, V.N. Khatri, R.K. Dutta, Performance of multi-edge skirted footings resting on sand, Indian Geotechnical Journal 48 (2018) 510-519. DOI: https://doi.org/10.1007/s40098-017-0270-6

[20] T. Gnananandarao, V.N. Khatri, R.K. Dutta, Pressure settlement ratio behavior of plus shaped skirted footing on sand, Journal of Civil Engineering (IEB) 46/2 (2018) 161-170.

[21] T. Gnananandarao, R.K. Dutta, V.N. Khatri, Model studies of plus and double box shaped skirted footings

resting on sand, International Journal of Geo-Engineering 11 (2020) 2.
DOI: https://doi.org/10.1186/s40703-020-00109-0
[22] V. Panwar, R.K. Dutta, Numerical study of ultimate bearing capacity of rectangular footing on layered sand, Journal of Achievements in Materials and Manufacturing Engineering 101/1 (2020) 15-26. DOI: https://doi.org/10.5604/01.3001.0014.4087
[23] Z. Szypcio, K. Dołżyk, The bearing capacity of layered subsoil, Studia Geotechnica et Mechanica XXVIII/1 (2006) 45-60.
[24] B. Davarcia, M. Orneka, Y. Turedia, Model studies of multi-edge footings on geogrid-reinforced sand, European Journal of Environmental and Civil Engineering 18/2 (2014) 190-205. DOI: https://doi.org/10.1080/19648189.2013.854726
[25] B. Davarci, M. Ornek, Y. Turedi, Analyses of multi-edge footings rested on loose and dense sand, Periodica Polytechnica Civil Engineering 58/4 (2014) 355-370. DOI: https://doi.org/10.3311/PPci.2101
[26] M. Ghazavi, S. Mokhtari, Numerical investigation of load-settlement characteristics of multi-edge shallow foundations, Proceedings of the 12th International Conference of International Association for Computer Methods and Advances in Geomechanics, Goa, India, 1-6 October 2008.
[27] M. Ghazavi, H. Mirzaeifar, Bearing capacity of multi-edge shallow foundations on geogrid-reinforced sand, Proceedings of the 4th International Conference on Geotechnical Engineering and Soil Mechanics, Tehran, Iran, 2-3 November 2010.
[28] V.N. Khatri, S.P. Debbarma, R.K. Dutta, B. Mohanty, Pressure-settlement behavior of square and rectangular skirted footings resting on sand, Geomechanics and Engineering 12/4 (2017) 689-705. DOI: https://doi.org/10.12989/gae.2017.12.4.689
[29] P.P. Das, V.N. Khatri, R.K. Dutta, Bearing capacity of ring footing on weak sand layer overlying a dense sand deposit, Geomechanics and Geoengineering (2019) (published online).
DOI: https://doi.org/10.1080/17486025.2019.1664775
[30] S. Alzabeebee, Dynamic response and design of a skirted strip foundation subjected to vertical vibration, Geomechanics and Engineering 20/4 (2020) 345-358. DOI: https://doi.org/10.12989/gae.2020.20.4.345
[31] IS 456, Indian standard code of practice for plain and reinforced concrete, (Fourth Revision), Bureau of Indian Standard, New Delhi, India, April, 2007.
[32] P. Pal, Dynamic Poisson's ratio and modulus of elasticity of pozzolana Portland cement concrete, International Journal of Engineering and Technology Innovation 9/2 (2019) 131-144.
[33] IS 800, Indian standard for general construction in steel – Code of Practice, (Third Revision), Bureau of Indian Standard, New Delhi, India, 2007.
[34] IS 6403 Code of practice for determination of breaking capacity of shallow foundations, Bureau of Indian Standard, New Delhi, India, 1981.